zation of $CF_2{=}CH_2$, the activation energy should be greater than 44 kcal/mol.

The activation energy for the dimerization of $CH_2{=}CH_2$ with $CH_2{=}O$ ($D\pi^\circ$ = 71 kcal/mol[1,5,17]) may be calculated from the reverse reaction[19] and thermochemistry.[5,15] This yields 54 kcal/mol, which suggests that the activation energy for the dimerization of $CF_2{=}CH_2$, with $D\pi^\circ$ = 62.5 kcal/mol, may be several kcal/mol greater than that for ethylene. Thus, with a reactivity considerably less than that of ethylene but a thermochemistry about the same, it is evident that, at temperatures where the thermal 2 + 2 cycloaddition reaction of $CF_2{=}CH_2$ will be fast, the equilibrium will favor the monomer so that the thermal dimerization (at ordinary pressures) is not expected.

These considerations show that the high values for the πBDE in 1,1-difluoroethylene confirmed in this work are qualitatively consistent with the reactivity of this olefin in addition reactions.

Acknowledgments. The authors gratefully acknowledge the support of this research by the National Science Foundation under Grant No. CHE 74-22189.

References and Notes

(1) S. W. Benson, *J. Chem. Educ.*, **42**, 502 (1965).
(2) J. M. Pickard and A. S. Rodgers, *J. Am. Chem. Soc.*, in press.
(3) E. C. Wu and A. S. Rodgers, *J. Phys. Chem.*, **78**, 2315 (1975).
(4) J. M. Pickard and A. S. Rodgers, *J. Am. Chem. Soc.*, preceding paper in this issue.
(5) J. D. Cox and G. Pilcher, "Thermochemistry of Organic and Organometallic Compounds", Academic Press, New York, N.Y., 1970.
(6) D. R. Stull, Ed., "JANAF Thermochemical Tables", The Dow Thermal Laboratory, Dow Chemical Co., Midland, Mich., 1970.
(7) M. G. Evans and M. Polanyi, *Trans. Faraday Soc.*, **34**, 11 (1938).
(8) H. S. Johnston, "Gas Phase Reaction Rate Theory", Ronald Press, New York, N.Y., 1966.
(9) S. W. Benson and G. R. Haugen, *J. Am. Chem. Soc.*, **87**, 4036 (1965).
(10) K. R. Maltman, E. Tschuikow-Roux, and K. H. Jung, *J. Phys. Chem.*, **78**, 1035 (1974).
(11) E. C. Wu and A. S. Rodgers, *J. Am. Chem. Soc.*, **98**, 6112 (1976).
(12) J. M. Tedder and J. C. Walton, *Acc. Chem. Res.*, **9**, 183 (1976).
(13) J. R. Lacher, G. W. Tompkin, and J. D. Park, *J. Am. Chem. Soc.*, **74**, 1693 (1952).
(14) A. Wilson and D. Coldhamer, *J. Chem. Educ.*, **46**, 549 (1963).
(15) S. W. Benson, F. R. Cruickshank, D. M. Golden, G. R. Haugen, H. E. O'Neal, A. S. Rodgers, R. Shaw, and R. Walsh, *Chem. Rev.*, **69**, 279 (1969).
(16) A. S. Rodgers, *J. Phys. Chem.*, **71**, 1996 (1967).
(17) D. M. Golden and S. W. Benson, *Chem. Rev.*, **69**, 125 (1969).
(18) (a) B. Atkinson and A. B. Trentworth, *J. Chem. Soc.*, 2082 (1953); (b) J. N. Butler, *J. Am. Chem. Soc.*, **84**, 1393 (1962).
(19) S. W. Benson and H. E. O'Neal, *Natl. Stand. Ref. Data Ser., Natl. Bur. Stand.*, **No. 21** (1970).

Interaction of Hydrogen, Carbon, Ethylene, Acetylene, and Alkyl Fragments with Iron Surfaces. Catalytic Hydrogenation, Dehydrogenation, Carbon Bond Breakage, and Hydrogen Mobility

Alfred B. Anderson

Contribution from the Chemistry Department, Yale University, New Haven, Connecticut 06520. *Received November 24, 1975*

Abstract: Interactions of hydrocarbons with iron surfaces are analyzed with theoretical calculations. The catalyzed breakings of carbon-carbon, carbon-hydrogen, and H_2 bonds are demonstrated. The interactions of hydrogen and carbon atoms with an iron atom on the surface weaken iron-iron bonds. Calculated geometries for ethylene and acetylene bonded to single iron atoms are similar to those in complexes. On the surface these molecules tend to dissociate into CH_2 and CH fragments. These in turn dehydrogenate with low activation energies calculated to be in the order of 20 kcal/mol. Adsorption energies for the hydrocarbons depend to a considerable extent on the iron 4s and 4p atomic orbitals, which stabilize the lowest lying σ framework hydrocarbon orbital.

I. Introduction

There is need for interplay between theory and experiment in the burgeoning field of surface chemisorption and catalysis. Neither experimental nor theoretical studies have given anything more than a rudimentary characterization of geometric structures and electronic and vibrational properties of surface systems. Even less is known about reaction mechanisms in surface catalysis. From the current experimental end, combinations of LEED, photoemission, work function, and electron induced ion desorption and flash desorption studies can lead to reasonable guesses of overlayer species and structures, on single crystal faces. Some infrared studies of species adsorbed to supported microcrystalline metal catalysts and thin metal films have shown shifts in adsorbate bond stretching frequencies due to interactions with the metal. Infrared techniques are not yet sensitive enough for use with single crystal faces. Despite the lack of unequivocal spectroscopic techniques for use in surface studies at present, data are being gathered, using the above techniques, by many laboratories. These data are pieces of a puzzle of concern to the experimental workers and to those wishing to develop theoretical procedures for understanding and predicting surface phenomena.

In this paper hydrocarbon interactions with iron are studied theoretically. There is only limited information about structures, absorbate energy levels, reaction pathways, and reaction activation energies of hydrocarbons on iron surfaces. In this paper model molecular orbital calculations are presented using one to five iron atoms. The important orbital interactions between adsorbates and these clusters are displayed and discussed. Changes in the positions of the energy levels are depicted as functions of geometric distortions of adsorbate molecules. Energy curves for HH, CC, and CH bond breaking are calculated. The ability of iron to catalytically break and form these bonds is demonstrated and discussed.

The theory[1] has two steps. First, rigid atoms are superimposed and the Hellmann-Feynman force formula is used to

Table I. Ground States, Equilibrium Bond Lengths, and Force Constants for First Transition Series Metal Diatomic Hydrides[a]

	ScH	TiH	VH	CrH	MnH	FeH	CoH	NiH	CuH	ZuH
State	$[^3\Phi]$	$[^4\Delta]$	$[^5\Delta]$	$^6\Sigma^+$	$^7\Sigma$	$[^4\Delta]$	$^3\Phi$	$^2\Delta$	$^1\Sigma^+$	$^2\Sigma$
R_e, Å					1.722	[1.61]	1.542	1.4754	1.4625	1.5945
ω, cm^{-1}				1581	1102.5	$[2.04 \times 10^3]$	~1890	~2000	1384.38	1607.6

[a] Proposed properties are in square brackets. Experimentally determined ones are from ref 13.

calculate two-body repulsive energies, which are summed. These energy components contain important information about bond stretching force constants and atomic radii.[2] Each component is the calculated electrostatic interaction between the nucleus of the less electronegative atom with charges on the other rigid atom. Then the atomic charge densities are allowed to relax, creating an attractive binding energy component. The relaxation is accomplished computationally by writing down molecular orbitals and diagonalizing the Fock matrix due to (approximately) superimposing the atomic Fock potentials. Rather than evaluating the energy due to charge redistributions with the Hellmann-Feyman formula, it is much easier to sum the orbital energies. The total orbital energy is added to the repulsive energy.

The molecular orbital wave functions employ atomic orbitals which are variationally determined or fitted to highly accurate self-consistent-field atomic orbitals.[3] The energy matrix employs, approximately, the eigenvalues of the corresponding atomic orbitals for the diagonal elements.[4] For the off-diagonal elements their average is multiplied by $2.25S \exp(-0.13R)$ where S is the atomic orbital overlap integral and R is the internuclear distance. The one-electron molecular orbital procedure is related to and justifies the extended Hückel approximation.[1]

This new theoretical procedure has been used to calculate structures and analyze the bonding properties of group 4A molecules and solids,[2] clusters of Ti, Cr, Fe, and Ni atoms,[5] van der Waals dimer molecules,[6] acetelyene and ethylene chemisorption to Ni(111)[7] and Fe(100)[8] surfaces, $Ni(CO)_4$, $Fe(CO)_5$, and $Fe_2(CO)_6$ C_2H_2 complexes,[9] and for an orbital analysis of 1,3 sigmatropic shifts on Pd films.[10] It is a generally useful approximate procedure and is the least expensive all valence electron theory for calculating good estimates of molecular structures, binding energies, force constants, and electron orbital energy levels. It overestimates atomic charges and should always be tested on diatomic species before treating larger molecules.

Experience shows, see ref 1, 2, 5-9, that the forte of the method is the determination of molecular structures, the important orbital interactions, and the approximate relative positioning of orbital energy levels. Because of the lack of self consistency, bond strengths for different classes of molecules, that is, covalent, ionic, or in between, are subject to systematic error. However, the activation energies estimated in this paper are believed to be significantly realistic because the systematic errors attendant to the adsorption of a molecule to the metal atoms should be constant enough when the molecule is subsequently distorted in geometry. Further, it will be seen that HH, CC, CH, FeH, and FeC bond lengths and energies are of good accuracy, so systematic errors are small. The basic orbital interactions between adsorbates and metals have been reviewed in model studies.[11] The parameters used in this paper are taken from ref 2 and 5 and are in a table comprising the Appendix to this paper.

II. FeH

Diatomic iron hydride has not been spectroscopically characterized but neighboring transition metal hydrides have been, allowing for extrapolation of FeH properties. These properties are to be used as a check of atomic Fe and H parameters used in the theory.

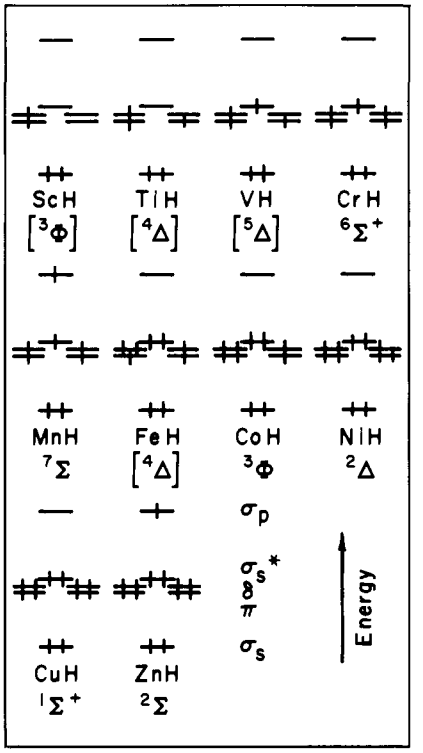

Figure 1. Relative energy levels, proposed orbital occupation schemes, and ground state symbols for first transition series metal diatomic hydrides. Proposed states are in square brackets. Experimentally determined states are from ref 13.

Experimentally known[13] ground state designations, bond lengths, R_e, and vibrational frequencies, ω_e, for diatomic hydrides of Cr, Mn, Co, Ni, and Zn are shown in Table I. Figure 1 shows the probable electronic configurations for the molecules. The information in the table and the reasoning behind the assignments in the figure bear discussing, for it is possible to draw conclusions about FeH from them.

The bond length for CrH is unknown, but the frequency of vibration is higher than for MnH, suggesting a shorter ond because of the theoretical relationship between force constants and atomic charge densities.[12] The MnH bond is about 0.2 Å longer than those of later hydrides in the series and its vibrational frequency is much smaller. Consistent with these facts as well as the spin multiplicities are the orbital occupation assignments in Figure 1. The high-spin MnH presents a half-filled shell situation with sufficient electronic stability to populate the high-lying σ_p orbital with one electron. The result of half-filling this high-lying orbital is the long MnH bond. Skipping on to CoH, the $^3\Phi$ state can be understood by doubly occupying the σ_s* orbital, which lies a few tenths of an electron volt, or less, above the d levels, to give the highest possible orbital angular momentum. It is no longer favorable in this non-half-filled shell system to have an electron in the σ_p orbital. The $^2\Delta$ state of NiH comes from adding another electron to

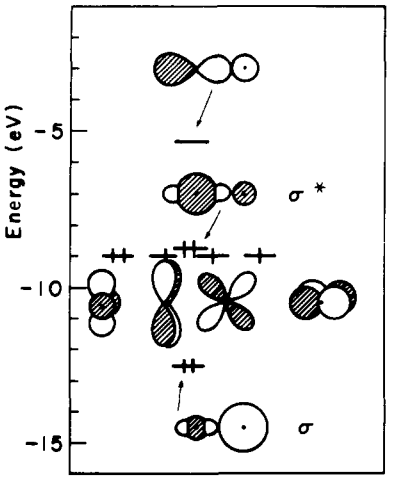

Figure 2. Orbital energy levels and orbitals calculated for FeH.

the weakly bonding π levels, filling them. With this the NiH bond length is 0.07 Å shorter than the CoH bond. CuH has a $^1\Sigma^+$ ground state due to adding an electron to the nonbonding δ set, filling it. The CuH bond is only 0.01 Å shorter than the NiH bond. The bond in $^2\Sigma$ ZnH is 0.13 Å longer because one electron must go into the σ_p orbital.

If the change in bond length on putting an electron in the σ_p level is 0.13 Å, then, compared to MnH, FeH, in the probable $^4\Delta$ ground state, should have a bond length of 1.59 Å. But since an electron has gone into a d level, this should decrease to 1.58 Å. On the other hand, compared to CoH, there is one less π electron so the bond length should be 1.61 Å. A range of 1.58–1.61 Å for the bond length seems reasonable for the $^4\Delta$ state of FeH.

By similar reasoning, the ground state designations are predicted for ScH, TiH, and VH in Table I and Figure 1. Since the effect of occupying the σ_s* orbital is unknown, bond lengths for these hydrides are not estimated here.

In order to calculate a vibrational potential energy curve for FeH with a bond length of about 1.6 Å and a frequency of about 2000 cm^{-1} and a reasonable $Fe^{\delta+}$ $H^{\delta-}$ ionic character, where δ is less than 1, the hydrogen valence state ionization energy can be raised by 2.5 eV from −13.6 to −11.1 eV and the 1s orbital exponent then is increased from 1.0 to 1.2 au. The predicted bond length and frequency in Table I are close to the expected values. The Fe parameters are taken directly from the cluster study.[5]

The 2.5 eV shift up in energy of the H 1s level could have been replaced with a smaller shift up and a small shift down of the Fe levels. This does not change the molecular orbital energy level orderings, shown in Figure 2. Because calculated atomic levels in Fe^+ drop only about 2 eV compared to Fe while for first row atoms the drop is around five times as much,[3] it is possible to assign the adjustment to H and, in a later section on FeC, to C. A detailed study of the photoemission spectra for chemisorbed and condensed acetylene and ethylene on Fe(100) surfaces shows no shifting of the orbital energy levels is necessary. See ref 8. Furthermore the binding and reaction energy curves presented later in this paper are little changed. The only major change is an increase in calculated adsorption energy when atomic orbital energy levels are not changed. Since no p orbitals were included in the H basis set, the π and δ orbitals for FeH shown in Figure 2 are degenerate. In reality, the π orbitals lie slightly beneath the δ orbitals, because of mixing with the p orbitals on H.

When the electrons in FeH are assigned to the molecular orbitals in a low-spin configuration, calculated properties change only slightly, as shown in Table II. This is fortunate because it is desirable to use a low-spin approximation for problems of adsorbates on iron clusters[5] in later sections. The calculated FeH bond energy of 41 kcal/mol is in the area of 63 kcal/mol known for CuH.[13]

Table II. Calculated Bond Lengths, Frequencies, and Dissociation Energies for the Proposed $^4\Delta$ Ground State FeH Molecule and for the Low-Spin $^2\Delta$ State

	$^4\Delta$	$^2\Delta$
R_e, Å	1.61	1.60
ω_e, cm^{-1}	2.04×10^3	2.13×10^3
D_e, eV	1.76	2.00

Table III. Calculated Bond Length, Force Constant, and Dissociation Energy for H_2[a]

	Calcd		Exptl
R_e, Å	0.74	0.77	0.741
k_e, mdyn/Å	7.83	6.58	5.71
D_e, eV	9.63	7.55	4.75

[a] Experimental values are from ref 13. The second column of calculated numbers corresponds to the H valence ionization energy being raised 2.5 eV.

III. Hydrogen Chemisorption, Mobility, and Effect on Iron Bonds

Iron and other transition metals can be very porous to hydrogen and, in the presence of hydrogen, either dissolved in the metal, or in the surrounding atmosphere, cracks in the strained metal may propagate readily.[14] Hydrogen is thermally mobile on metal surfaces. Various aspects of the interaction of hydrogen with iron are considered in this section.

The H_2 molecule is expected to bond dissociatively on an iron surface with a certain activation barrier.[14] By using the H parameters from the previous section, the properties of H_2 have been calculated and are found to be in agreement with experiment, as shown in Table III. In calculations of H_2 on Fe clusters and in calculations involving other adsorbates the calculated, not experimental, geometries will be used in evaluating overall adsorption energies. Calculations are performed with H_2 interacting with two Fe atoms spaced 2.866 Å apart, representing a fragment of the (100) surface. Numerous calculations involving various adsorbing species show, insofar as structures and energy levels are concerned, nothing is gained in using larger clusters of Fe atoms to represent the surface. The major surface–adsorbate interactions are highly localized. This localization has been recognized in other work in chemisorption of H_2 to Cu_2 and Ni_2 models of surfaces.[15] Long-range interactions between adsorbates are not a topic for this paper, though to study them large clusters would need to be used. As will be seen later, the strength of surface–adsorbate bonding depends quantitatively, but not qualitatively, on cluster size and geometry. See ref 6, 7, and 8 for further discussions of model size.

As the H_2 molecule approaches the Fe atoms in various orientations a weak state of nondissociative bonding is attained, as shown in Figure 3. The 2σ bridging position is slightly preferred, with a binding energy of 15.0 kcal/mol. Least preferred, by only 1.8 kcal/mol, is the one-coordinate perpendicular position. The H_2 molecule should be extremely mobile on the Fe surface.

The binding of H_2 to the surface is caused almost exclusively by a stabilization of the H_2 σ orbital by Fe 4s orbitals with some interesting antibonding 4p hybridization. Starting with H_2 at equilibrium, 2.7 Å from the surface in the 2σ position, a re-

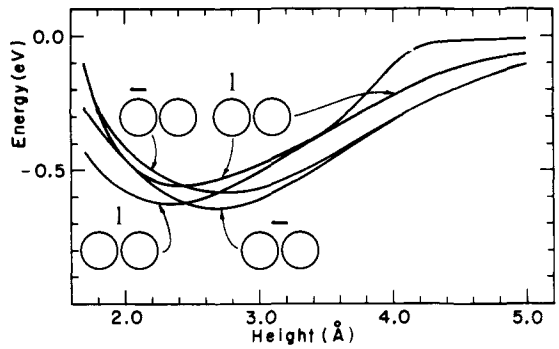

Figure 3. Binding curves for H_2 on two Fe atoms spaced 2.866 Å apart, representing a part of the (100) surface. The H_2 bond length is 0.77 Å, the calculated distance for free H_2.

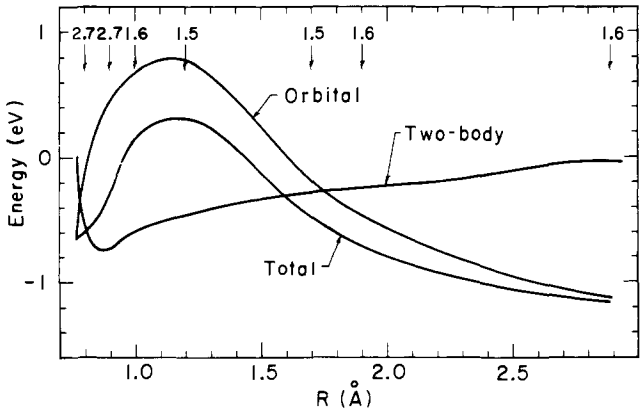

Figure 4. Energy as a function of H_2 bond length for H_2 in the σ position above two Fe atoms. Numbers at the top indicate the distance from H to the Fe surface. Two-body and orbital energy components are shown.

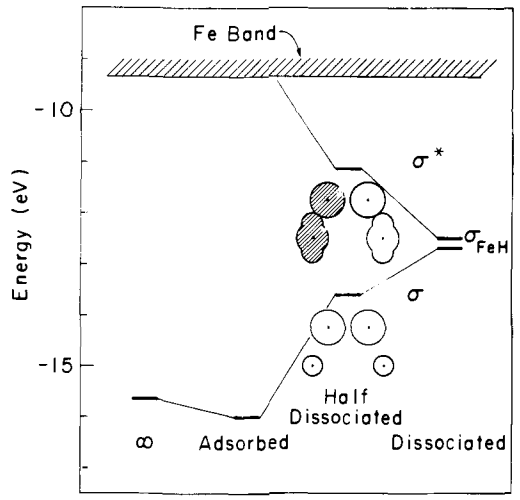

Figure 5. Orbital energy levels for H_2 dissociatively chemisorbing to two Fe atoms from the (100) surface. Shown is the bottom of the Fe s-d band of energy levels as based on Fe_2. This lowers somewhat for larger clusters. See ref 5. The band width for Fe_2 is about 1 eV and for a nine-atom cluster is about 3 eV, as shown in ref 5.

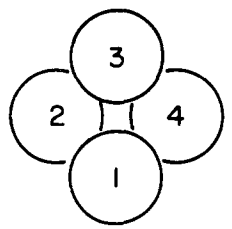

Figure 6. A fragment of bulk iron. Atoms 1 and 3 (or 2 and 4) make a part of the (100) surface. The distance between 1 and 2, for example, is the bulk distance, 2.482 Å. The distance between 1 and 3 is 2.866 Å.

action pathway for dissociation, the total energy, and two-body and orbital components are shown in Figure 4. It is seen that the two-body H_2 repulsion energy drops rapidly and the orbital energy rises rapidly as the H_2 bond is stretched. The total energy rises steeply. When the H_2 distance is about 1.0 Å, the molecules fall to 1.6 Å from the surface. As the total energy rises to a maximum this distance drops to 1.5 Å. When the H_2 bond is stretched to about 1.7 Å the total energy has dropped substantially due to the formation of bonding orbitals with Fe as shown in Figure 5. At this point the two-body repulsion energy between H and Fe causes an adjustment of H to 1.6 Å from the surface, which is the final value. This distance is the same as in diatomic FeH; a study of bond lengths between surfaces and adsorbates to greater resolution than 0.1 Å is not made in this paper.

With respect to the adsorbed molecular state, the activation energy to dissociative chemisorption is calculated to be 23 kcal/mol. With respect to the gas phase it is calculated to be 7.4 kcal/mol comparing favorably with an experimental determination of 6.8 kcal/mol.[14] The total binding energy of 27 kcal/mol for dissociative chemisorption from the gas phase compares well with the experimental value of 32 kcal/mol.[16]

Once dissociated, the H atoms are likely to vibrate about one-coordinate sites, as the energy in the bridging position rises 6.0 kcal/mol. However, this low activation energy allows for easy thermal mobility. Whether the dissociated H atoms would stay on nearest neighbor Fe atoms is a problem not treated in this paper. Such a treatment would require much larger clusters. In order to give an indication of how results depend on the particular model chosen, binding energies and H charges for H bonded to the 1 and 2 postions of the (100) surface fragment

Table IV. Binding Energies and Charges on H for H Bonded to Various Fe Clusters 1.6 Å from the Nearest Fe Atoms in the Low-Spin Approximation

Cluster description	Energy, eV	H charge
Fe atom	2.00	−0.36
Fe_2	2.00	−0.42
Fe_4 square	2.28	−0.40
Fe_4, No. 1, Figure 6	1.50	−0.46
Fe_4, No. 2, Figure 6	0.72	−0.27

in Figure 6 and other fragments are displayed in Table IV. Since the first four entries all use models of the (100) surface layer, it is seen that results are model dependent. The last entry suggests that there is a significant barrier for H entering the four-coordinate holes to penetrate the surface layer. Of course the H may cause a relaxation of the surface iron bonds, allowing them to stretch normal to the surface and making the entry of H easier.

Hydrogen embrittlement may be discussed in terms of FeFe bond strengths which in turn may be related to overlap populations. When an H atom is put 1.6 Å above an atom in an Fe_2 fragment from the (100) surface, the overlap population drops from 0.30 to 0.23 between the Fe atoms. When in the slightly less stable bridging position, 1.75 Å from each Fe atom, the overlap population remains 0.30. When placed midway between the Fe atoms, a situation accompanied by a rise in energy of 42 kcal/mol, the overlap population drops to 0.25. The overlap populations for the four-atom bulk cluster in Figure 6 are 0.41 and 0.04. With H on atom 1 the overlap of 1 on 2 and

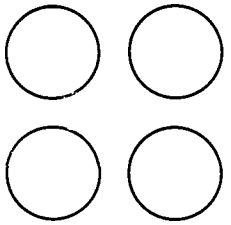

Figure 7. Four-atom Fe square from the (100) surface. The interatomic distance is 2.866 Å on an edge.

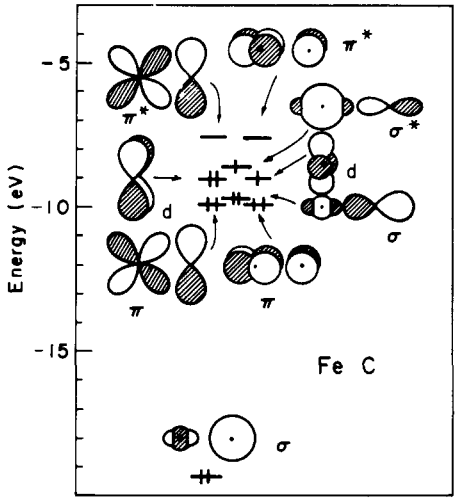

Figure 8. Energy levels and orbitals for FeC at the calculated bond length of 1.77 Å.

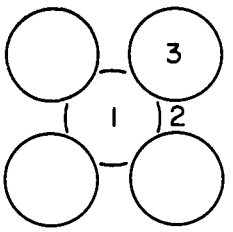

Figure 9. Four-atom Fe(100) surface fragment with one atom from the first layer beneath the surface at a distance of 2.482 Å from each surface atom, the bulk distance.

3 is 0.31 and 0.12, while the overlap of 2 on 3 and 4 is 0.42 and −0.01. When H moves to the center, a process requiring an input of 60 kcal/mol, the overlaps are 0.26 and −0.06. In a four-atom square from the (100) surface, as in Figure 7, the overlaps are 0.34 and 0.06. With H on a corner atom they are 0.22 and −0.11 with this corner atom; the others change much less. The net result is that when H is bonded to an Fe atom the bond order of that atom with its neighbors drops by about a quarter of its value.

The bond weakening between Fe atoms with H adsorption is a result of rehybridization of Fe atomic orbitals; the FeH bonds are formed at the expense of the Fe-Fe bonds. Although oxygen and, as will be seen in the next section, carbon also weaken the Fe-Fe bonds when adsorbed, O_2 actually arrests fracture propagation in an H_2 atmosphere[14] probably by forming a surface oxide which blocks the adsorption of additional hydrogen. Furthermore, if lattice defects are important to fracture, H atoms should find it quite easy to percolate along them if longer than bulk Fe-Fe bonds are associated with defects. Stress gradients might aid H transport to the developing crack, should bulk-dissolved H be important.[14]

IV. FeC

Diatomic iron carbide has not been reported spectroscopically. A study of the oxides, similar in format to the transition metal hydride study in an earlier section, suggests FeC, being isoelectronic to CrO, might have the same $^5\pi$ ground state.[13] The configuration would be $\sigma^2\pi_u^4\sigma^2d^2\sigma^1\pi_g^1$. However, orbital interactions are much greater in FeC than in FeO because of the small orbital exponents on C. This drives up the π_g level possibly out of reach of the ground state. If this is true, the ground state is likely a $^3\Delta$ corresponding to a $\sigma^2\pi_u^4\sigma^2d^3\sigma^1$ configuration, as shown in Figure 8. Adding one more electron to this produces the $^2\Sigma$ state observed for RhC.[13]

On raising C ionization energies by 2.5 eV, the predictions for the $^3\Delta$ and low-spin state seen in Table V are obtained. The bond length of 1.77 Å compares well with the $[Fe_6C(CO)_{16}]^{2-}$ FeC bond length of 1.82 Å.[17] It is fortunate to the study of chemisorbed hydrocarbons in later sections that precisely the same parameter adjustments can be made for C as for H and that the low-spin approximation seems to be accurate.

A C atom binds about 1.75 Å above an atom in Fe_2 with a calculated binding energy of about 115 kcal/mol. On immediately passing over a barrier of 3 kcal/mol, it falls to a point midway between the Fe atoms, about 1.8 Å from each of them, with a binding energy of 129 kcal/mol. In the one-coordinate position the Fe-Fe overlap population drops from 0.30 to 0.17 and in the bridging position it drops to 0.09.

On one-, two-, and four-coordinate positions of an Fe_4 square, as in Figure 7, arrangement from the (100) surface the binding energies are 123, 146, and 148 kcal/mol, where in the four-coordinate position C is coplanar with the Fe atoms. Although FeFe bonds are weakened in a manner similar to when H is adsorbed, certain FeFe bonds are strengthened.

On the five-atom cluster in Figure 9 the binding energies for the one-, two-, and four-coordinate positions are calculated to be 94, 111, and 79 kcal/mol, where in the four-coordinate case the C atom is 2.0 Å above the atom in the next layer below the surface. Binding in the four-coordinate position may be weakened because of the high, around 2, positive charge on the center Fe atom due to the cluster truncation. A large cluster on a charge iterative calculation might settle the question. In Table VI it is seen that there is a dependence of binding energy on position and iron cluster geometry, but a value of 4-6 eV brackets the range in binding energy.

A noticeable feature of Table VI is the large gain in Fe-cluster binding energy over diatomic FeC for the two- and four-atom Fe clusters. The strong bonding between C and the Fe clusters arises because of the nearness of the C valence levels to the s-d band of Fe levels and because of the availability of C p orbitals for greater possible bonding interactions with Fe d orbitals than was the case for H. The calculations show the bond order between Fe and the central Fe atom in the five-atom cluster can increase 30% when C is absorbed in a one- or two-coordinate position on the other side of the square. A study with larger Fe clusters could allow the determination of the range of influence of a single C atom and allow an understanding of C-C interactions.

V. Fe + C_2

The behavior of C_2 on an Fe surface is pertinent to the study of ethylene and acetylene, to the interaction of adsorbed C atoms, and to the study of Fe interactions with bulk carbon. C_2 has been discussed using the present theoretical method elsewhere.[4] Calculated and experimental properties are displayed in Table VII. When the C valence electron ionization energies are raised 2.5 eV, the C_2 molecular orbital energy levels rise, the C_2 bond stretches 0.06 Å, and the bond weakens.

In Figure 10 binding energy curves for C_2, with the calculated bond length from Table VII, but with the new atomic

Table V. Calculated Bond Length, Force Constant, Dissociation Energy, and Charge for FeC in the Probable $^3\Delta$ State and in the Lowest Spin Configuration

	$^3\Delta$	Low spin
R_e, Å	1.77	1.77
k_e, mdyn/Å	5.72	5.91
D_e, eV	4.27	4.65
Charge on C	−0.86	−1.09

Table VI. Binding Energies and Charges on C for C Bonded to Various Positions on Fe Clusters in Figures 6, 7, and 9 as Well as on Fe_2 and Fe in the Low-Spin Approximation

Cluster description	Energy, eV	C charge
Fe atom	4.65	−1.09
Fe_2, one coordinate	5.0	−1.20
Fe_2, bridging	5.6	−0.74
Fe_4, square, one coordinate	5.3	−1.21
Fe_4, square, two coordinate	6.3	−0.74
Fe_4, square, four coordinate	6.4	−0.64
Fe_5, one coordinate	4.1	−1.21
Fe_5, two coordinate	4.8	−0.85
Fe_5, four coordinate	3.4	−0.70

[a] FeC distances are near 1.8 Å and are discussed in the text.

Table VII. Calculated and Experimental Bond Length, Force Constant, and Dissociation Energy for C_2 Taken from Reference 2[a]

	Calcd		Exptl
R_e, Å	1.27	1.33	1.24
k_e, mdyn/Å	15.7	11.0	12.2
D_e, eV	7.89	4.09	6.16

[a] The second column of calculated numbers corresponds to the C valence ionization energies being raised 2.5 eV.

valence ionization energies, approaching Fe_2 are shown. The σ bridging position is favored by 26% over the perpendicular orientations and by 64% over the one-coordinate parallel orientation. In the σ orientation, the C_2 bond stretches spontaneously to a length of about 1.5 Å with an additional energy stabilization of 2%. On further stretching, a barrier of about 7 kcal/mol is encountered and then the atoms separate to give an overall binding energy of 143 kcal/mol. This might drop to around 171 kcal/mol as the C atoms drop into bridging positions, according to the previous section. The behavior of the total energy and the energy components is shown in Figure 11. Here the FeC distance is maintained at 1.8 Å. As the CC two-body energy drops the orbital energy rises, resulting in the barrier. On further stretching, the two-body energy is practically constant while the orbital energy drops. The orbital energy levels accompanying the breaking of the C_2 σ and π bonds and the forming of the FeC σ and π bonds are shown in Figure 12.

The catalytic dissociation of C_2 on Fe might, because of the small activation energy, be expected to occur at low temperatures spontaneously. Furthermore, strong interactions are expected between atoms in solid carbon fragments and iron surfaces.

VI. Fe + CH

The interaction of diatomic CH with iron should give information about hydrogenation and dehydrogenation reactions. CH is well represented in the calculational procedure,

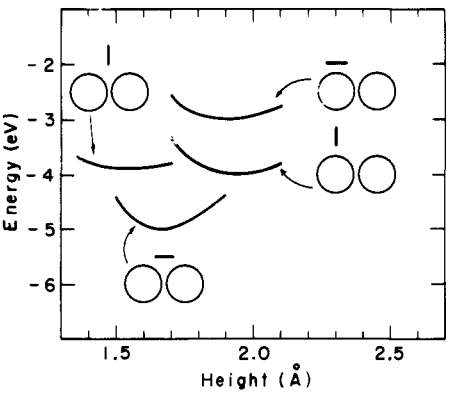

Figure 10. Binding curves for C_2 and two Fe atoms spaced 2.866 Å apart, representing a part of the (100) surface. The C_2 bond length is 1.27 Å, the calculated distance for free C_2.

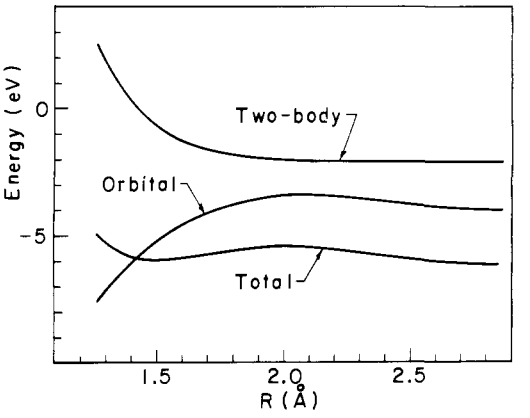

Figure 11. Total energy and components for C_2 stretching and dissociating on two Fe atoms in the σ orientation. The FeC bond length is maintained at 1.8 Å.

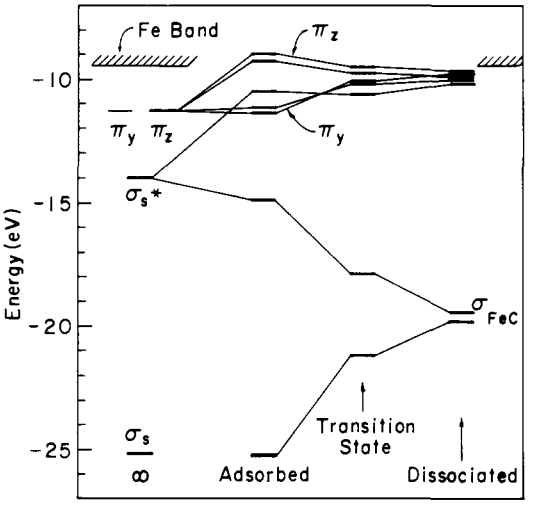

Figure 12. Energy levels for C_2 and Fe_2 during stages of adsorption and dissociation.

as seen in Table VIII. The molecular orbital energy level diagram and orbital pictures are shown in Figure 13. Of note are the p lobe from the σ_p orbital on the back side of C and the two π orbitals available for binding to Fe.

Calculations of CH interacting with a single Fe atom show attraction and a preference for the colinear orientation. When this geometry is used, the overlap population between Fe and H is negative. The reason for the stability of the colinear orientation lies in the strong interaction between the Fe's orbital

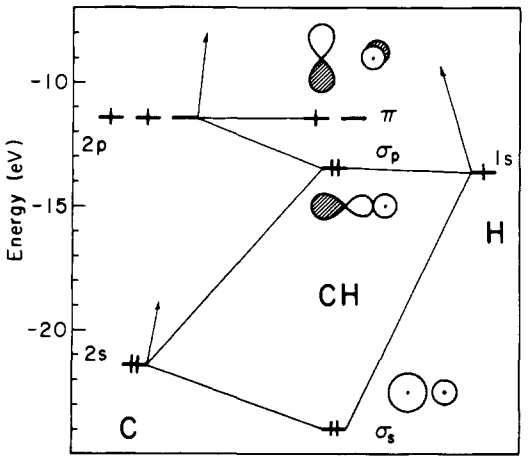

Figure 13. Calculated energy levels and orbitals for CH.

Table VIII. Calculated Bond Length, Force Constant, and Dissociation Energy for CH[a]

	Calcd		Exptl
R_e, Å	1.16	1.23	1.12
k_e, mdyn/Å	5.16	3.23	4.48
D_e, eV	3.07	1.33	3.47

[a] Experimental values are from ref 13. The second column of calculated numbers refers to C and H valence ionization energies being raised 2.5 eV.

and the σ_p CH orbital, which is diminished as CH is bent over. The symptomatic increase in magnitude of the negative FeH overlap is a general behavior for CH and larger molecules on Fe surfaces.

The calculated binding energy for CH to Fe_2 is 135 kcal/mol in the bridging position and 131 kcal/mol in the one-coordinate position, when the free CH calculated distance of 1.15 Å is used. The FeC distances are 1.9 and 1.7 Å, respectively. CH should be very mobile on Fe surfaces at low temperatures. However, at higher temperatures it is unstable.

To place CH in the bridging position parallel to the surface at the lowest energy, 1.6 Å above the surface, costs 26 kcal/mol. On stretching, a 6 kcal/mol barrier is reached at about 1.6 Å, with CH raised slightly to 1.7 Å high. As dissociation proceeds the H is adjusted to 1.6 Å high and the C is kept at 1.7 Å. The final energy is 132 kcal/mol about the same as for CH perpendicular to the surface. However, the C atom is expected to fall into a bridging or form coordinate position with a new total energy of about 146 kcal/mol. The energy curves for this catalyzed dissociation are shown in Figure 14 and the energy levels are shown in Figure 15. Almost precisely the same results have been calculated with an Fe_2 spacing of 2.482 Å, representing a fragment of the (211) and other surfaces. When CH is placed in the bridging position and bent over while the bend is stretched an activation energy to dissociation of 33 kcal/mol is found. This probably represents an approximate upper limit for activated CH bond breaking in Fe complexes and on Fe surfaces for unsaturated hydrocarbons. This is because most of the activation energy arises from tipping the CH bond over before any stretching has begun. In more saturated species than CH there will already be some tipping at the start.

VII. Fe + CH_2

Singlet methylene is calculated to have a HCH angle of about 120° and a bond length of 1.16 Å. The experimentally determined bond angle is 102°.[18] Orbitals and energy levels

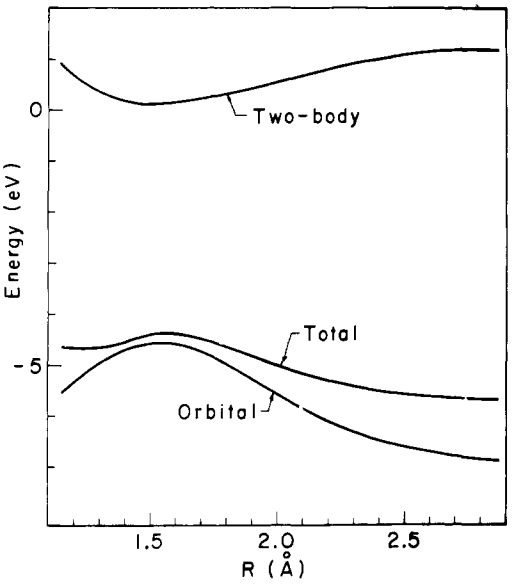

Figure 14. Total energy and components for CH stretching and dissociating on two Fe atoms in the σ orientation. The height above the surface is maintained at 1.7 Å.

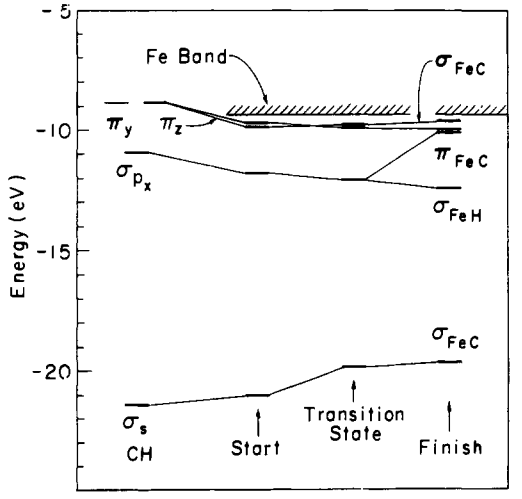

Figure 15. Energy levels for CH and Fe_2 during stages of adsorption and dissociation.

at the calculated geometry are shown in Figure 16. When the C and H valence state ionization energies are raised 2.5 eV, the calculated bond angle remains about 120° and the CH bond length increases 0.05Å, a typical change for this study.

As might be expected, CH_2 bonds C end first in the one-coordinate position on Fe_2. The FeC distance is 1.85 Å and the binding energy is 105 kcal/mol. The energy rises only 4 kcal/mol when methylene is turned over as in Figure 17, 1.7 Å from the surface. A barrier of 15 kcal/mol occurs when the CH bond parallel to the surface is stretched at 1.7 Å from the surface. When the dissociation is complete, and CH and H are adjusted to their orientations determined in earlier sections, the total binding energy is 128 kcal/mol. If CH drops into a bridging position this could increase to 132 kcal/mol.

When moved over to the two-coordinate position the binding energy decreases by 17 kcal/mol at the optimal distance of 1.4 Å. However, when CH_2 is rotated 90°, allowing strong interactions with the empty p orbital, the binding energy increases 5 kcal/mol at a distance of 1.5 Å from the surface. On the Fe surface CH + H is about 22 kcal/mol more stable than CH_2

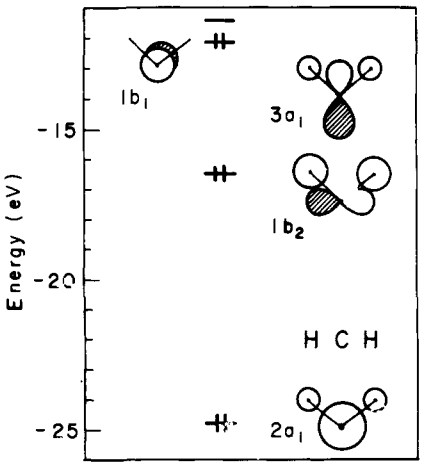

Figure 16. Calculated orbitals and energy levels for methylene at the calculated bond angle of 120° and bond length of 1.16 Å.

Table IX. Calculated Bond Lengths for Acetylene[a]

	Calcd	Exptl
R_e(CH), Å	1.15	1.056
R_e(CC), Å	1.31	1.204

[a] The experimental values are taken from C. D. Hodgman, Ed. "Handbook of Chemistry and Physics", Chemical Rubber Publishing Co., Cleveland, Ohio, 1962.

Table X. Energy Levels for Acetylene[a]

Orbital	Calcd, eV		Exptl,[b] eV
π^*	7.35	5.74	
π	13.66	10.66	11.4
σ_p	16.46	13.09	16.36
σ_s^*	20.79	17.40	18.38
σ_s	27.91	24.49	

[a] The second column of calculated numbers has the H and C valence ionization energies raised 2.5 eV. [b] D. W. Turner, C. Baker, A. D. Baker, and C. R. Brundle, "Molecular Photoelectron Spectroscopy," Wiley, London, 1970.

and C + H is about 20 kcal/mol more stable than CH.

Before going on to CH_3 and CH_4, it is possible to consider acetylene and ethylene. These species dissociate into CH and CH_2 fragments, which may then dehydrogenate as in this section and the previous one.

VIII. Fe + C_2H_2

Acetylene is calculated to have bond lengths close to the experimentally determined values, as seen in Table IX. The molecular orbitals and energy levels may be seen in Figure 18. These geometries are the ones used in this study when the H and C valence ionization energies are raised 2.5 eV even though previous experience suggests the bonds would, on energy minimization, stretch about 0.06 Å. When these valence ionization energies are moved up 2.5 eV, the energy level spectrum appears to become much improved, as seen in Table X, but actual levels may lie lower because photoemission spectra are influenced by shifts due to electronic relaxation.

Acetylene is attracted to a single Fe atom. The CC bond stretches 0.15 to 1.45 Å and the CH bonds bend up 30°. The binding energy is 63 kcal/mol. The FeC distance is 2.033 Å. This compares well with CC bond length increase of 0.12 Å and FeC distance of ~2.1 Å for $Fe_2(CO)_6$(RCCR) where R is a *tert*-butyl group.[19]

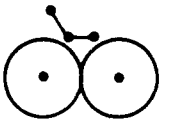

Figure 17. Position of methylene at start of dehydrogenation.

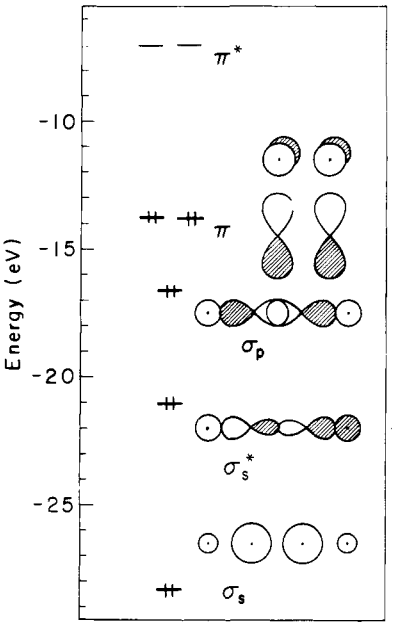

Figure 18. Calculated orbitals and energy levels for acetylene.

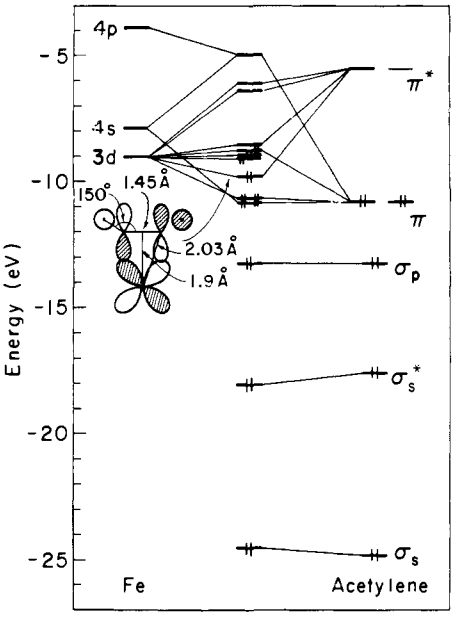

Figure 19. Molecular orbital energy level diagram for an Fe atom, acetylene, and acetylene bonded as shown to Fe.

The bonding interactions shift the molecular orbital energy levels as shown in Figure 19. Because of the bond stretch, the π levels do not shift down. Notable stabilization favoring bending occurs when the π^* orbital mixes in as shown in Figure 19. The π level, on mixing with Ni surface orbitals containing predominately 4s character, shifts down about 1 eV.[20,7] Will the same happen with Fe?

Placing acetylene on Fe_2 in a one-coordinate orientation parallel to the FeFe bond results in approximately the same bond lengths and angles as above and a binding energy of about

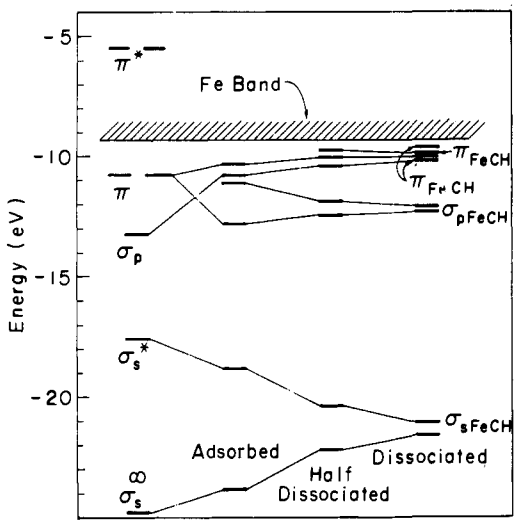

Figure 20. Molecular orbital energy level diagram for acetylene dissociating on two Fe atoms spaced 1.866 Å apart. The adsorbed position corresponds to a C-C bond length of 1.7 Å and the half-dissociated position corresponds to 2.3 Å.

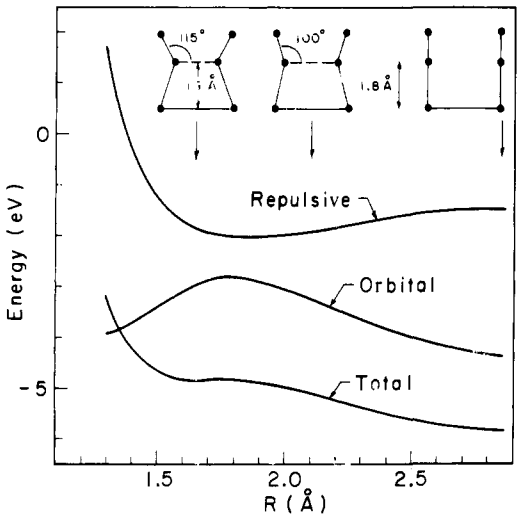

Figure 21. Total energy and components for acetylene dissociating on two Fe atoms 2.866 Å apart.

76 kcal/mol. When placed in the σ bridging position, acetylene dissociates into two CH fragments with zero activation energy, according to the calculations. The energy levels at four stages of this dissociative chemisorption are depicted in Figure 20. On dissociation the FeCH orbitals show about 0.5 eV or less splitting due to their interaction. The total binding energy for the dissociated acetylene is 135 kcal/mol with the CH fragments in adjacent one-coordinate positions. About 8 kcal/mol stabilization would be expected for the CH fragments falling into bridging positions, according to section VI. The energy changes and geometry changes for this reaction are shown in Figure 21. Acetylene may be slightly stable on a cold Fe surface with a bond stretch of 0.35 Å and an HCC angle of 115°. The weak barrier may occur when the bond is stretched an additional 0.1 Å.

Once dissociated, the CH fragments can themselves dissociate. There is experimental evidence for liberation of H_2 on adsorption of acetylene on the Fe(100) surface and the photoemission spectrum is complicated, suggesting various species may be present on the surface.[21,8]

A considerable amount of heat is liberated as acetylene dissociatively chemisorbs. Whether or not CH dissociates should depend on the initial surface temperature, the rate at which acetylene is adsorbed, and the rate at which the metal surface can conduct heat to lower temperature regions.

Since the calculations show dissociation on two Fe atoms, the same will happen on larger clusters, and this is observed.[8] However the orientation of acetylene, or ethylene in the next section, during dissociation might be different on a larger cluster. Many calculations on larger clusters show in fact the strongest bonding interaction occurs for the σ orientation above two nearest neighbor Fe atoms. Hence the Fe_2 model is justified in this paper. The effect of larger clusters is to shift binding energies and adsorbate ionization energies but the figures in this paper would look much the same, with a widening of the Fe s-d band from around 1 eV to about 3 eV. See ref 8 for results on larger clusters and comparison with recent experiments which corroborate this work. See also ref 7 for a discussion of acetylene and ethylene on Ni(111) where similar geometries are found but the interaction with the surface is weaker, as comparison with experiments corroborates again.

Table XI. Calculated Bond Lengths and Angles for Ethylene[a]

	Calcd	Exptl
R_e(CH), Å	1.17	1.086
Re(CC), Å	1.5	1.337
∠HCH, deg	120	117.3[b]

[a] The experimental values are taken from footnote *a*, Table IX. [b] H. F. Schaefer III, "The Electronic Structure of Atoms and Molecules," Addison-Wesley, Reading, Mass. 1972.

Table XII. Energy Levels for Ethylene.[a]

Orbital	Calcd, eV		Exptl, eV
π^*	8.88	6.93	
π	13.06	10.19	10.51
a_{2g}	15.27	12.07	14.4 (7)
b_{1g}	15.85	12.72	12.38
b_{2u}	16.96	13.55	15.6 (8)
b_{3g}	22.13	18.74	18.8 (7)
a_{1g}	27.33	23.86	

[a] The second column of calculated numbers has the H and C valence ionization energies raised 2.5 eV. The experimental numbers are from footnote *b*, Table X.

IX. Fe + C_2H_4

The agreement between calculated and measured geometry for ethylene is good, as seen in Table XI. Calculated and experimental ionization energy levels are shown in Table XII. Orbital pictures and energy levels are shown in Figure 22.

Ethylene binds to a single Fe atom with an energy of 66 kcal/mol. The CC bond stretches 0.15 to 1.65 Å. When the HCH angle is kept equal to 120°, the HCH plane bends up 30° away from Fe. The FeC distance is 2.16 Å. In the two Fe complexes (C_2H_3CN) $Fe(CO)_4$[22] and $(C_2H_2CO_2H)$ $Fe(CO)_4$[23] the CC bond stretches 0.06 Å and the FeC distance is 2.10 Å, a reasonable check. The bending up of the CH bonds occurs for similar reasons as for acetylene, as may be seen in Figure 23. The π level shifts down 0.2 eV.

When adsorbed in the bridging position the CC bond stretches 0.30 Å to a calculated length of 1.8 Å. The CH bonds bend up 55° and the π level shifts down 1.4 eV. The A_{2g} level moves up 1.1 eV above the shifted π level. The interaction with Fe is much stronger than with the Ni(100) surface. Ethylene on Ni shows a 0.9 eV shift down of the π level and no noticable shift in the A_{2g} level.[7,20] The calculated energy levels for eth-

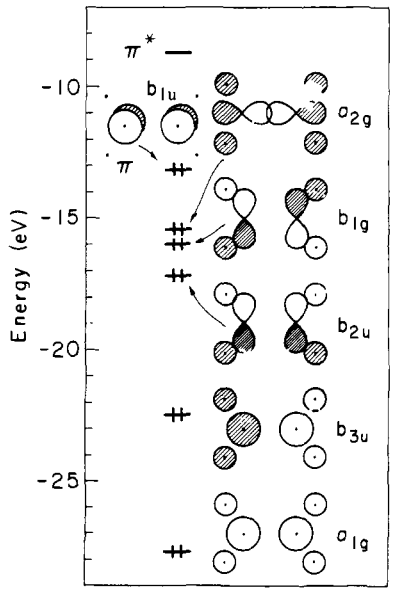

Figure 22. Calculated orbitals and energy levels for ethylene.

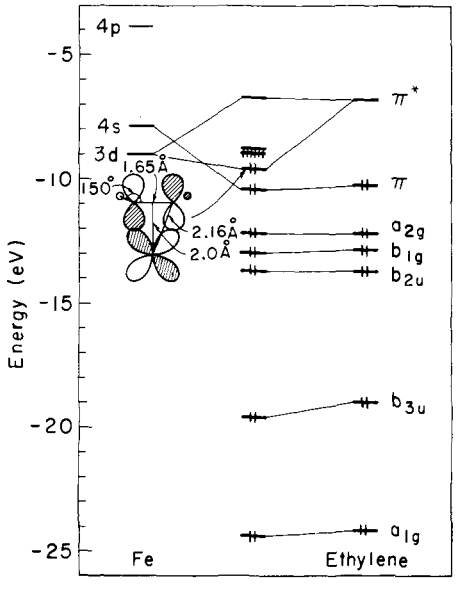

Figure 23. Molecular orbitals and energy levels for ethylene, an Fe atom, and ethylene bonded as shown to Fe.

ylene dissociating on Fe_2 are shown in Figure 24. The calculated binding energy for adsorbed ethylene is 109 kcal/mol.

The geometry changes and energy changes for ethylene dissociating are shown in Figure 25. A barrier of about 1 kcal/mol is found when the CC bond is stretched to about 2.0 Å. On complete dissociation the CH_2 fragments stand up in one-coordinate positions and the total binding energy is 116 kcal/mol. These methylene fragments can then dissociate if the surface is hot enough. The heat liberated on adsorption may dehydrogenate ethylene.[8]

X. CH_3 + Fe

Methyl dehydrogenates on Fe_2 with a calculated activation energy of 14 kcal/mol. The CH_2 + H products are more stable by 25 kcal/mol, assuming CH_2 drops into a bridging position. The calculated reaction path and energy changes are shown in Figure 26. The FeC distance in methyl is 2.1 Å and for methylene it is 1.9 Å. The overall binding energy of methyl to the two Fe atoms is 84 kcal/mol.

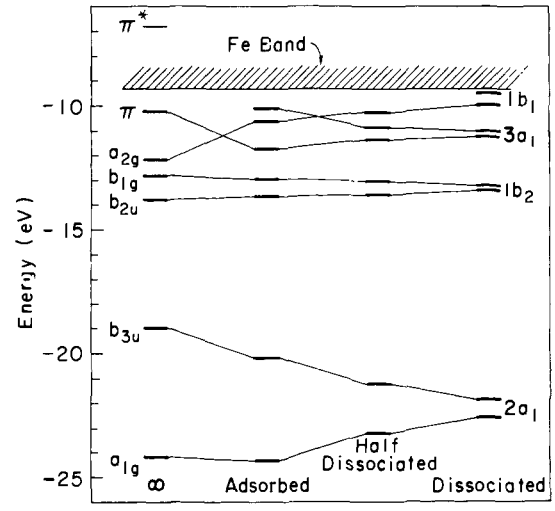

Figure 24. Molecular orbital energy level diagram for ethylene dissociating on two Fe atoms spaced 2.866 Å apart. The adsorbed position corresponds to a C-C bond length of 1.80 Å and the half-dissociated to 2.3 Å.

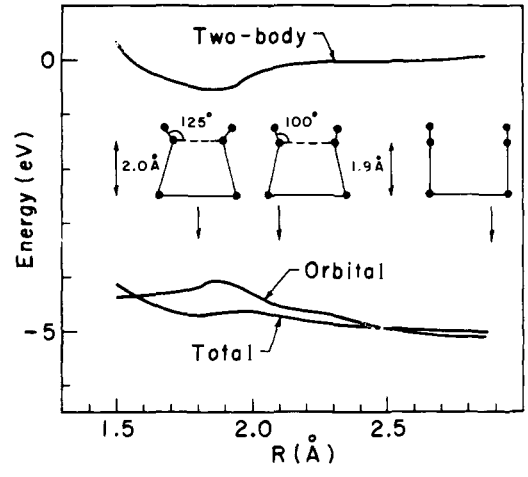

Figure 25. Total energy and components for ethylene dissociating on two Fe atoms 2.866 Å apart.

When moved over to the bridging position, the distance to the surface decreases to 1.8 Å and the binding energy decreases 8 kcal/mol. The empty p lobe bonds most favorably with a single Fe atom.

XI. CH_4 + Fe

On two Fe atoms, the dehydrogenation of methane to methyl is initially calculated to have a relatively high activation energy of 42 kcal/mol for a reaction path where, as CH_4 settles down on the surface with a CH bond perpendicular to the surface and pointed at an Fe atom, the H atom moves to a neighboring Fe atom. The energy gained due to dehydrogenation is 32 kcal/mol.

The calculated binding energy of CH_4 to the two Fe atoms is 43 kcal/mol and the FeC disance is 3.0 Å. When a CH bond points straight down at an Fe atom CH can easily role over to gain 3 kcal/mol with three CH bonds pointing down about an Fe atom and the FeC distance being 2.5 Å. On orientating methane so that a CH bond points toward the other Fe atom and a CH bond remains pointing straight up, new activation energy of about 21 kcal/mol is found for shifting the H atom over to the other Fe atom. This value is much closer to activation energies for CH bond breaking in methyl and methylene.

The 43 kcal/mol adsorption energy comes almost entirely

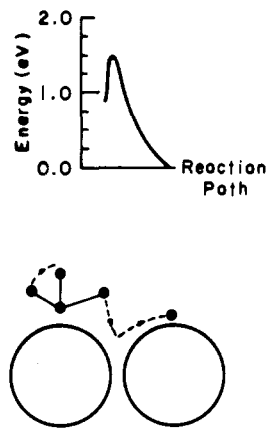

Figure 26. Calculated reaction pathway and energy change for CH_3 going to CH_2 + H on two Fe atoms spaced 2.866 Å apart. The Fe-C distance goes from 2.1 to 1.9 Å.

Table XIII. Calculated Activation Energy, E_a, and Heat of Reaction, E, for Dehydrogenation Involving the Loss of a Single H Atom

Species	E_a, kcal/mol	$-E$, kcal/mol
CH	32	20
CH_2	24	22
CH_3	14	25
CH_4	21	32

from the stabilization of the lowest σ molecular orbital in methane by interaction with 4s and 4p orbitals on Fe. The small orbital exponents for these orbitals make the orbitals diffuse, allowing for a large enough interaction with methane to cause the stabilization. If the exponent is not accurate, this would be reflected in the bond strengths between methane, and the other hydrocarbons in this study, with Fe. It would be necessary to adjust the exponents according to some criteria which are unavailable at present to change the magnitude of this effect.

XII. Discussion

It is impossible to review here the thousands of papers on transition surface chemisorption and metal catalysis, some of which stretch back in time to the past century. Excellent reviews exist on catalysis in organic chemistry;[24] theories and mechanisms of chemisorption and catalysis have been reviewed recently,[25-27] and many groups are now performing essentially reproducable experiments using clean single crystal faces.[27,28] One of the first things learned from ref 24-28 and other reviews is that iron and other transition metals adsorb and catalyze changes in structures of all the species discussed in this paper. However, with all the experimental unknowns regarding surface structures and compositions, the pertinance of carefully controlled single crystal surface studies and quantum mechanical calculations to finding and explaining synthetically useful catalysts may be questioned. Surely the pertinance will be realized slowly.

Surface science, which studies all structural and electronic properties of surfaces and adsorbates, has begun to characterize chemisorption and catalysis in a well-defined manner. For certain systems, such as atomic hydrogen monolayer coverage of silicon crystal faces, theory and experiment appear to have met with good agreement.[29] An approach to understanding, theoretically or experimentally, disordered surface systems is intrinsically more difficult.

This paper has addressed reactions on iron surfaces in the simplest way. Interactions between nonbonded adsorbates were omitted by including in the calculations only one reacting species. It is well known that the degree of coverage of a surface affects adsorption and activation energies.[26-28] Generally, the heat of chemisorption decreases as coverage increases, and changes in activation energies and pathways can result as well. In addition to these energy effects, the presence or absence of pertinent surface species can exert an entropic influence on surface reactions. These effects can be treated theoretically in the future.

In addition to leaving out neighboring adsorbate species and their influences, neighboring atoms in the surface and in the bulk were omitted.[30] This omission does not[8] change the specific analysis of the surface reactions treated here, but it can influence the magnitudes of energies calculated and the degree of shifting of energy levels.[5,7] The calculations of H and C on various sizes of iron clusters show the variation and, apparently, since the bonding interactions are quite localized, it is not wrong to discuss mechanisms and energies as calculated in terms of surface events.

Errors in the theoretical method due to the approximations it rests upon[1] appear to be well within bounds of usefulness. The calculated binding energies, structures, and force constants for the adsorbates are all accurate and the energies and geometries of interacting species should be qualitatively correct. The calculational uncertainties in bond lengths do not detract from the importance of calculated reaction pathways, activation energies, and valence ionization energies.

In the absense of experimental or exhaustive theoretical criteria for determining the 4p orbital exponent for iron, some question exists as to the correctness of the calculated magnitude of hydrocarbon adsorption energies. The calculated 43 kcal/mol adsorption energy for methane is inconsistant with the reported "slow" chemisorption on iron.[26] The 109 kcal/mol adsorption energy calculated for ethylene is larger than the reported value of 68.[26] It is tempting to subtract out some of the stabilization of the lowest σ framework orbited on mixing with the diffuse Fe 4s and 4p orbitals or make them less diffuse. This binding, which is due to the ability of an orbital field of 4s and 4p to interact with diffuse adsorbate orbitals, is, for closed shell adsorbates such as methane, a van der Waals binding. Its strength will vary with adsorbate, but there is a likelihood that when an adsorbate reaches distances to the surface where chemical bonds dominate, such as during the reactions considered in this paper, the influence of these orbitals on reaction pathways and activation barriers is small,

Table XIV. Parameters Used in This Paper

Atom	S			P			D		
	n^d	ζ^e	I^f	n	ζ	I	n	ζ	I
H^a	1	1.200	−11.10						
C^b	2	1.625	−18.90	2	1.625	−8.90			
Fe^c	4	1.600	−7.87	4	0.800	−3.87	3	C	−9.00

[a] The valence ionization energy is shown raised 2.5 eV. [b] The valence ionization energies are shown raised 2.5 eV from the usual values in ref 11. [c] From ref 5. The d orbital has two exponential components, the first with an orbital exponent 5.35 and a coefficient 0.536 59 and the second with an orbital exponent 1.8 and a coefficient 0.667 79. [d] Principal quantum number. [e] Slater exponent. [f] Ionization energy.

that is, the contribution to binding to the surface might be relatively small and constant. Thus the calculated reaction mechanisms and activation energies in this paper may be more accurate than the adsorption energies of CH_4, CH_3, CH_2, C_2H_2, and C_2H_4.

Activation and stabilization energies for dehydrogenation of CH, CH_2, CH_3, and CH_4 are shown in Table XIII. The activation energies to hydrogenation and dehydrogenation decrease on going from CH to CH_2 to CH_3. Energetically, C is the prefered surface species, and at high temperatures H desorbs. However, when H_2 is maintained at a sufficient pressure it can combine with surface carbon to form gases[25] and gasoline.[31] Statistical considerations will be important in determining what species exist on an iron surface at various temperatures and H_2 pressures. Once an alkane forms it is likely to desorb as its bond to the surface is much weaker than for the unsaturated hydrocarbons. Should two CH_3 fragments collide, ethane might desorb, and so on. The relationships between concentrations of surface species and temperature and pressure are thermodynamic problems beyond the reach of quantum chemistry as applied to the calculation of energy surfaces in this paper.

Acknowledgment. This research was supported by the National Science Foundation.

Appendix

The theory used in this paper is derived in ref 1. Further applications are in ref 2 and 4–9. Parameters used in this paper are in Table XIV.

References and Notes

(1) A. B. Anderson, *J. Chem. Phys.*, **62,** 1187 (1975).
(2) A. B. Anderson, *J. Chem. Phys.*, **63,** 4430 (1975), and references therein to past work by the same author.
(3) E. Clementi and D. L. Raimondi, *J. Chem. Phys.*, **38,** 2686 (1963); E. Clementi and C. Roetti, "Atomic Data and Nuclear Data Tables 14", Academic Press, New York, N.Y., 1974; J. W. Richardson, W. C. Nieuwpoort, R. R. Powell, and W. F. Edgell, *J. Chem. Phys.*, **36,** 1057 (1962); J. W. Richardson, R. R. Powell, and W. C. Nieuwpoort, *J. Chem. Phys.*, **38,** 796 (1963).
(4) W. Lotz, *J. Opt. Soc. Am.*, **60,** 206 (1970), and ref 3.
(5) A. B. Anderson, *J. Chem. Phys.*, **64,** 4046 (1976).
(6) A. B. Anderson, *J. Chem. Phys.*, **64,** 2266 (1976).
(7) A. B. Anderson, *J. Chem. Phys.*, **65,** 1729 (1976).
(8) A. B. Anderson, C. Brucker, and T. N. Rhodin, to be published.
(9) A. B. Anderson, *Inorg. Chem.*, **15,** 2598 (1976).
(10) A. B. Anderson, *Chem. Phys. Lett.*, **35,** 498 (1975).
(11) A. B. Anderson and R. Hoffmann, *J. Chem. Phys.*, **61,** 4545 (1974).
(12) A. B. Anderson, *J. Mol. Spectrosc.*, **44,** 411 (1972).
(13) B. Rosen, "Spectroscopic Data Relative to Diatomic Molecules", Pergamon Press, Oxford, 1970.
(14) R. A. Oriani, *Ber. Bunsenges. Phys. Chem.*, **76,** 848 (1972).
(15) H. Deuss and A. van der Avoird, *Phys. Rev. B*, **8,** 2441 (1973).
(16) D. O. Hayward, "Chemisorption and Reactions on Metallic Films", J. R. Anderson, Ed., Academic Press, New York, N.Y., 1971, Chapter 4.
(17) M. A. Churchill, J. Wormald, J. Knight, and M. J. Mays, *J. Am. Chem. Soc.*, **93,** 3073 (1971).
(18) G. Herzberg and J. W. C. Johns, *Proc. R. Soc. London, Ser. A*, **295,** 107 (1966).
(19) F. A. Cotton, J. D. Jamerson, and B. R. Stultz, *J. Organomet. Chem.*, **94,** C53 (1975).
(20) J. E. Demuth and D. E. Eastman, *Phys. Rev. Lett.*, **32,** 1123 (1974).
(21) T. N. Rhodin, private communication.
(22) A. R. Luxmoore and M. R. Truter, *Acta Crystallogr.*, **15,** 1117 (1962).
(23) C. Pedone and A. Sirigu, *Inorg. Chem.*, **7,** 2164 (1968).
(24) P. H. Emmett, P. Sabatier, and E. E. Reid, "Catalysis Then and Now", Franklin, nglewood, N.J., 1965.
(25) D. O. Hayward and B. M. W. Trapnell, "Chemisorption", Butterworths, London, 1964.
(26) G. C. Bond, "Catalysis by Metals", Academic Press, London, 1962.
(27) J. R. Anderson, Ed., "Chemisorption and Reactions on Metallic Films," Academic Press, New York, N.Y., 1971.
(28) G. Ertl and J. Kuppers, "Low-Energy Electrons and Surface Chemistry", Verlag Chemie, Weinheim *Bergstr.*, Germany, 1975.
(29) J. A. Appelbaum and D. R. Hamann, *Phys. Rev. Lett.*, **34,** 806 (1975).
(30) A localized Pauling bond energy-bond order model has been used with apparent success in explaining the dissociative chemisorption of ethylene on the Pt(111) surface. See W. H. Weinberg, H. A. Deans, and R. P. Merrill, *Surf. Sci.*, **41,** 312 (1974).
(31) E. E. Donath, *Adv. Catal.*, **8,** 239 (1956).

Optically Active Amines. 22.[1] Application of the Salicylidenimino Chirality Rule to α-Amino Acids

Howard E. Smith,*[2a] Elizabeth P. Burrows,[2a,3] Maurice J. Marks,[2a] Robert D. Lynch,[2a,4] and Fu-Ming Chen[2b]

Contribution from the Departments of Chemistry, Vanderbilt University, Nashville, Tennessee 37235, and Tennessee State University, Nashville, Tennessee 37203, and the Tennessee Neuropsychiatric Institute, Nashville, Tennessee 37203. *Received May 3, 1976*

Abstract: The sign of the Cotton effects near 255 and 315 nm in the circular dichroism (CD) spectra of the *N*-salicylidene derivatives formed in situ using sodium salicylaldehyde and chiral amine hydrochlorides, α-amino acids, and α-amino ester hydrochlorides correlates with their absolute configurations. The Cotton effects are generated by the coupled oscillator mechanism and their sign is the same as the chirality (right-handed screw for positive chirality) of the interaction of the dominant oscillator of the amine moiety with those of the salicylidenimino chromophore, the chirality of the interaction being deduced by conformational analysis.

The salicylidenimino chirality rule[5] correlates the absolute configurations of the *N*-salicylidene (**1a**) and *N*-5-bromosalicylidene (**1b**) derivatives (Schiff bases) of a wide variety of chiral primary amines with the sign of the Cotton effects near 255 and 315 nm in their circular dichroism (CD) spectra. Included are α- and β-arylalkylamines[5,6] and cyclic terpene[7] and steroidal amines.[1]

The electron (isotropic) absorption (EA) spectra of the

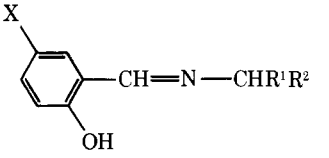

1a, X = H
b, X = Br